ANALYSIS OF CARBON DIOXIDE FLUX FROM A TOWER SENSOR IN ABISKO SWEDEN

STUDENT: QIAOYIN HE
SUPERVISOR: JOHAN LINDSTROM

Mathematical Statistics
Centre for Mathematical Sciences
Lund University

Abstract

This thesis focus on reporting and analyzing the influence factors to CO_2 flux, which is defined as the exchange of carbon dioxide between atmosphere and the ground, from a measuring tower which is located in Abisko national park. According to the footprint record, the CO_2 fluxes mainly comes from the surrounding sparsely populated forest or wetlands.

In addition to using the Eddy Covariance System to observe the fluxes of methane and carbon dioxide, the records also include atmospheric temperature, relative humidity, latent heat and sensible heat flux. The carbon dioxide flux observation fluctuated in a small range between -1.3~2.5 $\mu mol/m^2/s$ during the winter, and from -11.8 $\mu mol/m^2/s$ to around 7.5 $\mu mol/m^2/s$ in summer. Data shows highly correlations between the carbon dioxide flux and methane flux, temperature, and photosynthesis. The CO_2 flux always shows a negative correlation with the CH_4 flux, temperature, humidity, and photosynthesis.

This thesis investigates the possibility for separately predict the CO_2 flux from different land type but highlights many challenges during creating the divided models as well.

A Gaussian process model estimated using INLA with time parameter, air temperature and CH_4 flux shows the better fitting results. While the seasonal periodogram taken into the consideration, the prediction could be improved a lot according to the DIC and WAIC results. However, no matter which models in the thesis are used to predict, the sub flux from different type of land is still not easy to identify.

Key Words

Abisko, carbon dioxide flux, net ecosystem exchange, R-INLA, time series

Acknowledgements

For the study of my master's degree and completion of graduate thesis, I would like to thank the professor Johan Lindstrom for his distinctive idea, useful advice, and unwavering support. Besides, I would like to thanks to professor Natascha Kljun, who and her research group provided me with the research data of this thesis.

Moreover, I am really appreciating for all the people who have helped me during these two years, especially for Magnus Wiktorsson, the supervisor of our mathematical statistics, for his advice of my master study and supporting of my residence permit extension. Furthermore, I would like to thank for my bachelor supervisor Jianhua Lin, who always helped me to deal with some professional problems through jet lag when I did not know whom to turn to.

Although in the past two years my life and study were not so satisfied and well for most of the time, it is still experiencing an epidemic, even now the world is still experiencing an epidemic which makes the condition harder and more tough, finally I still made it through. I am very grateful to my parents for their financial and spiritual support to me. They used their rich experience and extremely professional career planning knowledge to accompany me out of confusion, pressure and worry every time.

Thanks for all my friends I met in Sweden. Besides helping me with schoolwork, they also went to the museum and the gym with me, making my life in a foreign country warmer and interesting.

Lund, June 2021
Qiaoyin He

Content

Chapter 1

Introduction

1.1 Background

According to the United Nation's report in 2019, the speed and severity of climate change have exceeded expectations. One of the most significant reasons for this is a greenhouse gas, carbon dioxide. Carbon dioxide has great impacts on climate, farmland, ocean acidification and many other aspects. As the result, doing research on carbon dioxide flux is of high importance.

The abnormal climate makes human beings encounter more and more survival problems. As a result, people are paying increasing attention to the subject of global environmental changes and the work of controlling carbon emissions these years. Since the 1990s, all parts of the world have gradually begun to establish continuous and long-term monitoring towers, which using eddy covariance measurements, to collect data of surface carbon dioxide, moisture, humidity, temperature, radiation, latent heat, sensible heat flux, and so on. The data obtained by these observatories is also the focus of research on regional climate, hydrology, and ecology. (Moncrieff *et al*. 1997, Aubinet *et al*. 2000).

In 1996, the first global monitoring network for surface carbon dioxide, water vapor, and thermal energy flow, called Fluxnet, was established in North and South America. (Baldocchi, D.D. et al., 2001) Subsequently, the AsiaFlux in Asia and CarboEuroFlux in Europe were established in 1999 and 2004 respectively. (Joon *et al*, 2010) According to incomplete statistics from Fluxnet in 2015, there are more than 440 measuring stations or towers of Fluxnet around the world, and this number is still increasing year by year. (Fluxnet history, https://fluxnet.org). The goal of Fluxnet is to understand the carbon dioxide flow, water and energy flow behaviors that control the earth's biosphere on time and space scales, and to provide information to help assess the net major productivity, evaporation and energy absorption in the ecosystem.

ICOS, whose full name is "Integrated Carbon Observation System", is a European Research Infrastructure focusing on the long-term qualification and analysis of the European continent's and neighboring regions' standardized and high-precision

measurement facilities and observations data of greenhouse gas balances. (www.icos-ri.eu). Atmosphere observation stations, ecosystem observation stations and ocean observation stations are three different components included in ICOS. Each of these stations is overseen by a Thematic Centre. Data from stations in the ICOS system are completed into a high-quality database that also included additional information from other national ecosystem observations and field stations.

1.2 Purpose and problem formulation

This paper uses the data from an Eddy covariance (EC) flux observation tower in Abisko, Sweden to monitor the carbon dioxide flux of flat afforestation land. The EC technique is used to measure and compute vertical turbulent fluxes inside atmospheric boundary layers (Baldocchi *et al* 1988, Verma 1990, Lee *et al* 2004), whose detail definition and mathematical foundations will be introduced in the next chapter. The purpose of this thesis is to classify and model the carbon dioxide flux of forest land and wetland using weights form on atmospheric transport model. The following questions will be answered in this thesis:

(a) The relationships between different variables;
(b) The seasonable pattern with in the variables;
(c) If a Gaussian model with time-series components can be used to separate observed fluxes into wetland and forest contributions.

1.3 Limitation and assumption

This paper mainly focuses on the variables that have significant influence on the CO_2 flux. Studies have shown that there is some correlation between carbon dioxide flux and radiation. However, because of some issues during the measurement, the observation data of radiation used in this paper makes no sense. Besides, because rather than last few years, the data used in this paper is the observations in 2016, the changes and human activities in these several years have not been taken into consideration. All of these may cause some deviations in the actual forecasting process.

Chapter 2

Literature review

In this section, some of the previous academic papers, practical reports and published books that are important to the subject will be reviewed, starting with the basic definitions, and the observation station that provides the data set of this thesis, a brief introduction of the Abisko national observation station, the different measurement methods used in different periods and conditions, and the Eddy covariance method which is used by the majority of contemporary observatories and also by the observatory from which the data in this thesis is derived are included in this chapter.

2.1 Wetland definition

The term "wetland" encompasses a wide range of meanings. The most frequently accepted worldwide definitions are divided into technical definitions and Ramsar Convention definitions, in addition to regional definitions may differ between countries. A wetland, according to Paul (2010), is a habitat created when water inundates soils, causing anaerobic and aerobic processes to dominate, requiring the biota, particularly rooted plants, to adapt to floods. In addition, on February 2nd,1971, the Ramsar Convention on Wetlands of International Importance, Particularly as Waterful Habitat was signed in Ramsar, Iran. "*Regions of marsh, fen, peatland, or water, whether natural or artificial, permanent or temporary, with water that is static or flowing, fresh, brackish, or salt, including areas of sea water whose depth at low tide does not exceed six meters.*" according to the definition. (the Ramsar Convention of 1971)

The wetlands included in the list of internationally important wetlands contains a total of 2,303 individual locations, with a total wetland area of 22,892,1972 hectares in accordance with the convention.

If distinguished following the formation of wetlands, it can be divided into two categories: natural wetlands and artificial wetlands. Among them, natural wetlands could be further divided into coastal wetlands and inland wetlands based on geographic regions. Artificial wetland refers to the traces left by human activities or ecological restoration, salt flats, paddy fields, reservoirs, ecological ponds, detention ponds, sand

dams for mountain streams, and various canals or ditches. The term 'wetlands', the land type used in this thesis, is much more closely associated with grassy marshes. Forested bogs and shrub swamp with higher than 30% vegetation cover are classified as "forests" in this thesis.

2.1.1 Abisko station

This thesis focuses on observations from Abisko, Sweden. The Abisko-Stordalen Palsa Bog station (ICOS code SE-Sto), where the observation data and information in this thesis come from, is located 10 kilometers east of Abisko in the 1100-hectare Stordalen natural reserve. Because the location is near the 0°C isotherm, permafrost in the mire is intermittent and quite dynamic. Permafrost has been found degrading in numerous places of the mires as a result of recent warming in the area. The site is a mixed palsa-mire with occasional permafrost that is rapidly thawing. Sedges and sphagnum mosses grow in the damp areas of the mire, while lichens and dwarf birch grow at the higher elevations.

The photo and map in Figure 2.2.1 show the observation data acquisition equpment and the location of the station respectively. (Photo, map, and the basic information all come from the ICOS official page, https://meta.icos-cp.eu/resources/stations/ES_SE-Sto)

Figure 2.1.1: Measuring Instrument

Figure 2.1.2 The location of the Abisko station

2.2 Comparison of observation methods

"Flux", refers to the physical quantity (mass, or energy) that passes through a unit area during unit time, which can be directly measured by observing instruments, and the actual value can be obtained. In the 1950s and 1960s, a group of scholars represented by Bowen Ratio began to use micrometeorology.

Two common observation methods are open path (OP) and closed path (CP). The location of the gas sampling and the optical analysis unit is the biggest difference between these two methods. This difference will have a series of effects on subsequent experimental design and data processing methods (Haslwanter *et al.*, 2009).

Chamber technique, which dates back to the 1990s (Moore & Knowles, 1990) and was developed in the early 21st century (Deborde *et al.*, 2010), is the most common method in CP (Mitsch *et al.*, 2014). Besides this method, the gradient method proposed by Simpson in 1997, and the relaxed eddy accumulation (REA) are also CP methods. However, the mainstream method for observing flux at this stage is the OP eddy covariance method (EC), which is also the method used to obtain the observations used in this thesis. (Hommeltenberg *et al.*, 2014; Morin *et al*., 2017)

As close-path and open-path are two completely different ways of working with observations and data collection, each of which have their own advantages and disadvantages, a comparison between them is necessary. To some extent, the open-path is a refinement on close-path. Under the close-path classification, there are three main methods: gradient, chamber, and random eddy current accumulation. The open-path, on the other hand, is mainly represented by the best known and most commonly used eddy covariance method.

For the close-path, both gradient and random eddy accumulation methods could record long-term and continuous observations and measure the flux data of a large area. The greatest advantage of chamber method over the former two, lies in the following three points: the fast speed to get the observations data, the easy principle of the operation, and the much cheaper equipment. With the same advantages, the gradient and random eddy accumulation methods also have several similar disadvantages, for example, the sampling line is susceptible to moisture which may lead to the bad measurements. Either the gradient method or the random eddy accumulation method needs large space to operate and has excessive power consumption. What is more, when using the

gradient method, the environment has a greater impact on the measuring instrument. However, for the chamber method, the equipment will disturb the sampling site by hindering the air flow. Besides, it is impossible to obtain long-term, continuous, and large spatial observations with the chamber method.
(Detto *et al,* 2011; Pumpanen *et al*, 2004)

2.2.1 Eddy covariance system

As a representative method under the OP classification, the advantages of EC are even more obvious. It has limited requirement on both space and power consumption. Moreover, the flux of a large area could be measured more accurately. However, the cost of the equipment is very high, especially compared with the other methods. Additionally, the instrument may also be influenced by the rain.
(Denmead, 2008; Morin *et al*, 2017)

The principle of Eddy covariance systems was first mentioned by Montgomery (1948) and Swinbank (1951). By the 1980s, the eddy covariate system (EC) had been developed to measure the mass or energy flux in the atmosphere (Baldocchi et al., 1988; Brut et al., 1998). It is a kind of micro-meteorological method used to observe the gas, energy, and momentum exchange between the atmosphere and ecosystem. It should be noticed that the vortex motion is irregular and random, and it has no meaning for the flux at a certain moment. Therefore, the change in the average flux of matter per unit time must be considered.

To understand how the EC system works, it should be recognized that all atmospheric gases move with the wind, so they seldom sit static. Although it appears that air moves horizontally across the earth, it really moves in spinning eddies. Friction causes the air to tumble as it moves. In other words, a horizontal flow of multiple spinning eddies can be visualized as air flow. The eddy element of the vortex covariance can be more visually represented in the figure 2.2.1 below.

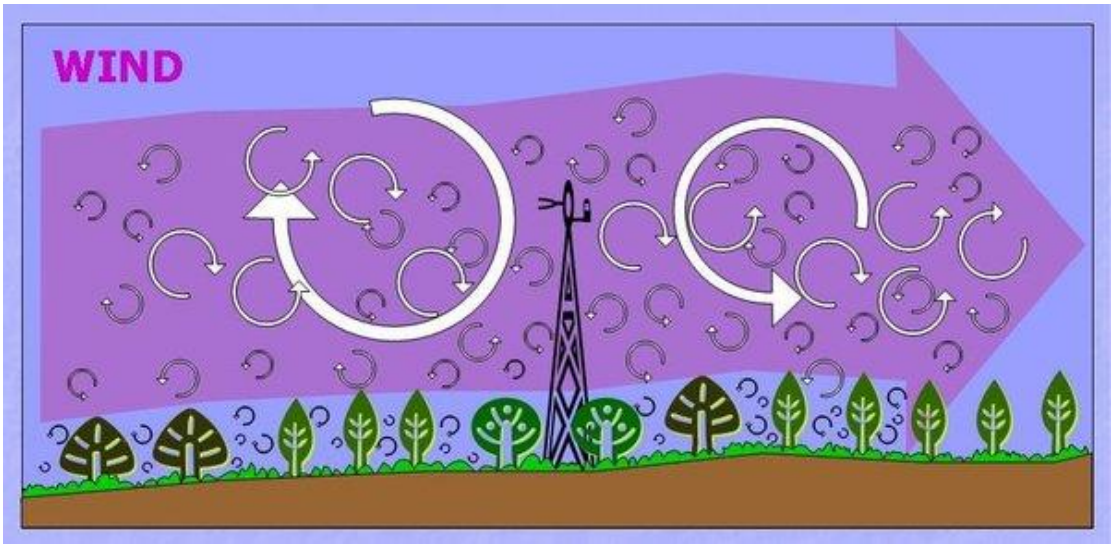

Figure 2.2.1: The eddy part of eddy covariance

(Lee X., Massman W., and Law B. 2004)

By rapidly measuring the movement of the gas at the time (Figure 2.2.2) and using knowledge of how the air panels move, scientists try to transfer the eddy movements to a horizontal flow of the gas. The EC measurements occur at a rate of 10 or more times per second. All this information is displayed in 30-minute increments and mapped across time. (Dave and Louis, 2018) The physical schematic could be seen as Figure 2.2.2.

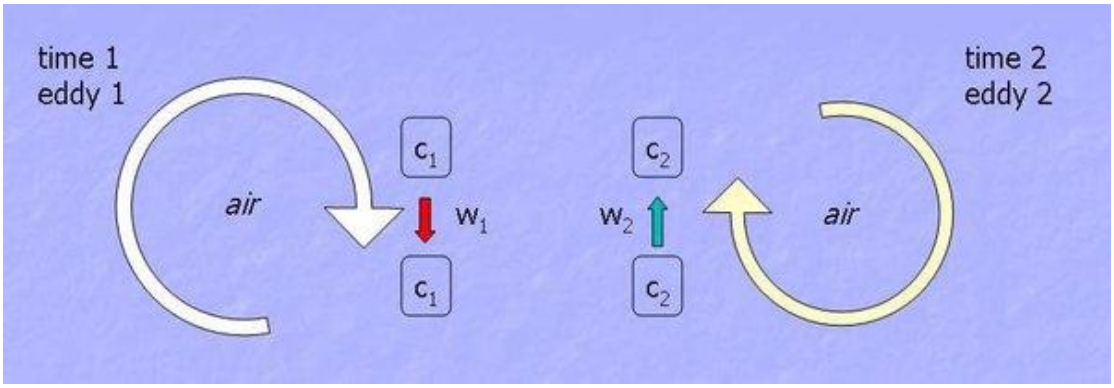

Figure 2.2.2: The physical schematic of eddy covariance method

(Lee X., Massman W., and Law B. 2004)

Chapter 3

Pipeline and Data pre-processing

3.1 Data pre-processing

In the process of data research, the general steps always follow the path of gathering data, processing them, simulating or estimating models, and comparing models. These steps could be further explained as follows.

Firstly, as the data used in this paper comes from the cooperative observation data of the Abisko atmosphere observatory and the ecological research group of Lund University, there are no ethical issues to consider.

In the part of pre-processing, the target of this step before simulating and analyzing models is to ensure the data is in a suitable format for the analysis.

(a) The original observations are divided into five groups according to the land types and normalized difference vegetation index (NDVI), which is a satellite measured indication if a target area includes living green vegetation. While in the data pre-processing, they are merged and reclassified into “wetland” and “forest”.
(b) Deleting data including invalid information and missing values.

3.2 variables in the flux dataset

The variables in the flux dataset used in this thesis are available in the Table 2.3.1. The original database was obtained from the Abisko ICOS station (2016).

Table 3.2.1: variables in the flux dataset (2016)

variables	Description
Fluxdata	
time	time slot in Matlab version
temp	air temperature
humidity	relative humidity
ppfd	the incoming radiation that vegetation can use for photosynthesis, however, the record is missing because of some machine reason
CH_4	methane flux in this dataset
GPP	gross primary production, for example photosynthesis
respiration	the respiration in the soil, plant, microorganisms and animal included
he	sensible heat flux
le	latent heat flux
NEE	net ecosystem exchange, in this data set is net CO2 flux
footprint (the classification parameters, used as weight)	
fw1	forest percentage, including both high and low NDVI
fw2	wetland percentage, including both high and low NDVI

3.3 data overview

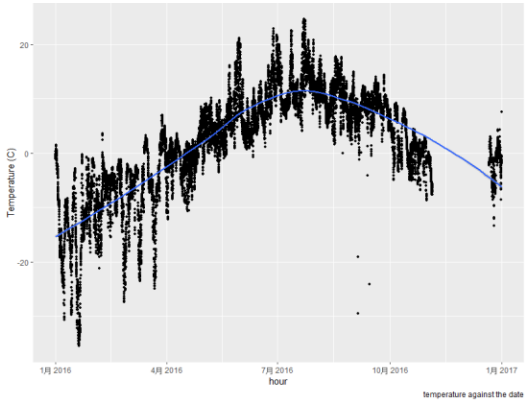

(a)temperature

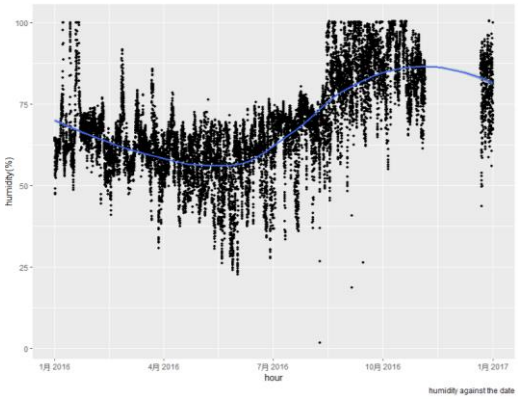

(b) relative humidity

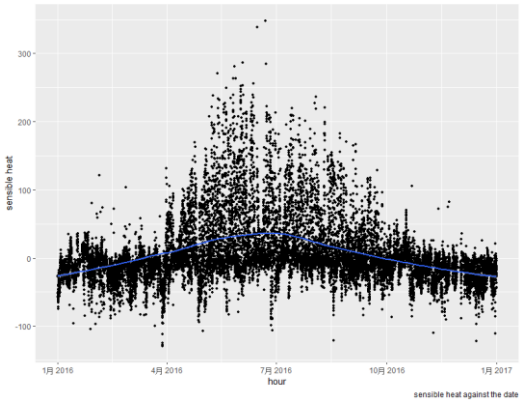

(c)sensible heat flux

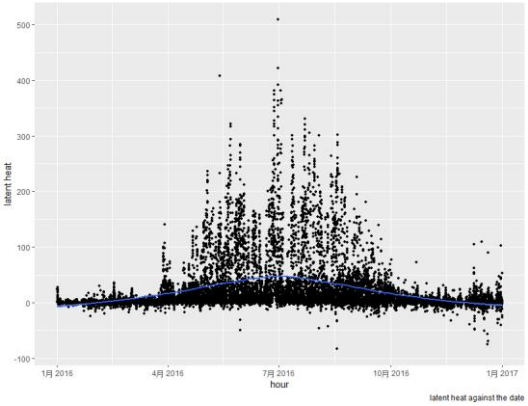

(d)latent heat flux

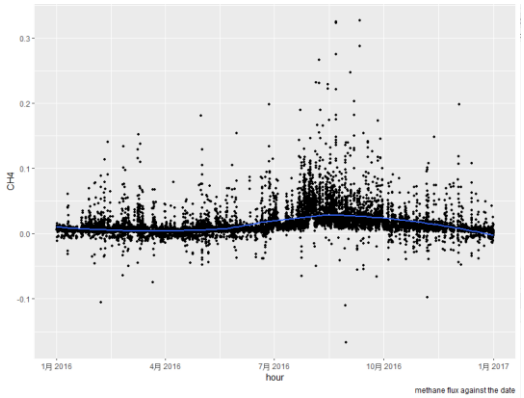

(e) methane flux

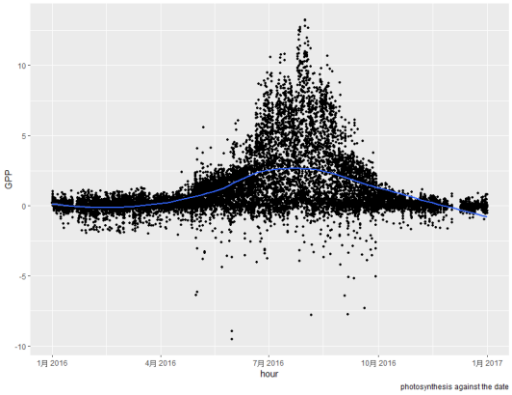

(f) photosynthesis

Figure 3.3.1: Variables against the time

The temperature and relative humidity during the observation period are shown in Figure 3.3.1. Table 3.3.1 shows the monthly average temperature and relative humidity during the observation period (2016).

It can be seen from the figure that the air temperature is divided into distributions

between -31.4 ~ 21.7℃. There are a few abnormal temperature values in September 2016, with temperature as low as -23℃. The temperature reached the highest value in a year between July and August, and then gradually decreases, reaching its lowest value in late January and early February.

The relative humidity is mainly distributed between 24.8%~100%. In addition to high humidity on rainy days, relative humidity and temperature are usually negatively correlated, with humidity being low during the day and high at night.

In addition, from the figure above, no matter the sensible heat or latent heat, the observation values in summer are more scattered compared with the winter. The same pattern also occurs in methane flux and photosynthesis. It's easy to see that with increasing temperature, the observation values of these four variables also become higher and are dispersed. For the sensible heat, it usually fluctuates between -120-50 J/g from October to April. Then the gap between the highest and lowest values gradually increased from April and reached at peak in middle of July, whose values could reach 450 J/g apart.

The change in methane flux in winter is concentrated between -0.15 and 0.2 $C/m^2/h$. However, rather than appearing in summer, the largest range of 2016 is in September and October, which contains from -0.17 ~ 0.34 $C/m^2/h$. It means that there is about two and a half months of phase shift between methane flux and temperature.

Table 3.3.1: monthly mean values of all variables

	Jan	Feb	Mar	Apr	May	Jun
Temperature(℃)	-13.8	-8.2	-5.6	-0.9	6.1	8.0
Humidity (%)	67.7	63.6	60.5	58.7	53.8	58.6
Latent heat (J/g)	0.1759	0.5925	3.8702	12.6884	44.9955	44.3845
Sensible heat (J/g)	-12.793	-15.359	-18.552	9.6803	38.8873	40.5472
Methane flux ($C/m^2/s$)	0.00672	0.00774	0.00665	0.00406	0.00816	0.0103
Photosynthesis	-0.0319	-0.0420	0.03573	0.19057	0.83375	1.91394
	Jul	Aug	Sep	Oct	Nov	Dec
Temperature(℃)	12.5	10.0	8.3	1.5	NaN	NaN
Humidity (%)	66.4	74.9	87.5	88.0	NaN	NaN
Latent heat (J/g)	45.6014	35.9858	16.7772	3.5594	0.8920	1.3718
Sensible heat (J/g)	28.6159	17.1633	-0.2629	-8.6260	-17.122	-22.347
Methane flux ($nmol/m^2/s$)	0.02419	0.03596	0.02459	0.01305	0.01158	0.0063327
Photosynthesis	3.40040	2.797576	0.86131	0.16355	NaN	NaN

(Due to some failure of measuring instruments and/or equipment maintenance, some observational data for November and December is missing.)

Chapter 4

Theory and Methodology

4.1 Regression

Regression models were introduced by Legendre in 1805 and Gauss in 1809 for the first time. Today, it is widely used in various fields such as sociology research, epidemiology. This estimating method is popularly used to explore relationships between an independent predictor and several dependent variables.

4.1.1 Standard regression

Suppose $y = (y_1, y_2, \ldots\ldots, y_n)$ is a sequence of observation data,

β_0 is the intercept,

$\beta = (\beta_1, \beta_{0,\ldots\ldots}, \beta_m)$ represent the effects of the independent variables,

$x = (x_1, \ldots\ldots, x_M)$ to be the covariates,

In ordinary regression, y_i is thought to be normal distribution: $y_i \sim Normal(\mu_i, \sigma^2)$. With the mean, μ, given by:

$$\mu_i = \beta_0 + \sum_{m=1}^{M} \beta_m x_{mi}$$

However, as standard regression analysis is usually applicable to regression model analysis where the relationship between variables is linear, it is inadequate in non-linear relationships, which are more general and common in real-world application problems. Before considering the extension and expand of standard linear regression, several specific definitions and interpretations need to be introduced.

4.1.2 Covariance function

Covariance is a measure of how much two variables change together, and the covariance function, or kernel, represents the temporal or spatial covariance of a random variable process or field. A covariance function $C(X(s_1), X(s_2))$ gives the covariance of the values of the random field at the two locations s_1 and s_2 for a random field or stochastic process $X(s)$ on a domain D.

The correlation of a signal with a delayed duplicate of itself at different delays is known as autocorrelation, or serial correlation in the discrete-time case. In time series, where time t_1 and t_2, replace the spatial location in s_i, $C(X(t_1), X(t_2))$ is also called the autocovariance function, which analysis is a mathematical technique for detecting patterns that repeat themselves. The autocorrelation of a real or complex stochastic process in statistics is the Pearson correlation between the values of that process at various times, which is a function of the time lags between the two time points. (Gubner, John 2006).

Suppose X_t is the value at time t, then the autocorrelation function between time slots t_1 and t_2 is defined as:

$$R_{XX}(t_1, t_2) = \mathrm{E}[X_{t1} * \overline{X_{t2}}]$$

where $\overline{X_{t2}}$ is the complex conjugation of X_{t2}.

4.1.3 Nonlinear regression

With the same notation as in section 4.1.1, a non-linear function of some covariates $f(z_i)$, where z_i are covariates that have a nonlinear effect on y, could be introduced. With this, the regression model can be expanded into a linear and a nonlinear parts as:

$$\mu_i = \beta_0 + \sum_{m=1}^{M} \beta_m x_{mi} + \sum_{l=1}^{L} f_i(z_{li})$$

The nonlinear terms $f(z_i)$ could presently be modeled in several ways, but in this thesis, we are going utilize splines that are based on a stochastic process or field representation that builds on a random walk.

4.1.4 Regression simulation with random fields

In the multivariate case, with the classification (geographical subdivision), the density function of random vector $x = (x_1^T, x_2^T, \ldots\ldots, x_n^T)^T$ with the simulation and the conditional expectation of the vector under the estimation at time t could be shown as:

$$y_t = x_t + e_t \quad with\ e_t \sim N\left(0, I_{\tau_e^{-1}}\right)$$

$$\mathrm{E}[x_t|y_t] = \left(\tau \mathrm{Q} + A^T I_{\tau_e} A\right)^{-1} A^T I_{\tau_e} y$$

$$= (\frac{\tau}{\tau_e} Q + A^T A)^{-1} A^T y$$

When considering the specific case of AR(1)-process, the vector with the x is time ordered depends only on the previous element. In other words, with all other elements are given, the random walk is defined by the conditional distribution follows:

$$x_t|x_{t-r} \sim N(x_{t-r}, \sigma^2)$$

$$x_t = x_{t-\mathrm{r}} + \varepsilon$$

where ε refers to the noise.

There are usually two kinds of situations under general condition:
Firstly, when the time slot $\tau \to \infty$, $\varepsilon \to 0$, the estimation based on every time points will show a flat trend, even approaching nearly a straight line in the extreme case.
Secondly, when the time slot $\tau \to 0$, $\varepsilon \to \infty$, the estimation line would have high fluctuations all the time.
The same as general case, with the $\frac{\tau}{\tau_e}$ goes to zero or infinity, the value of x_t would equal to y_t or $\bar{y}$ respectively.

The estimation at time t, using the notation y_t, could be written as:

$$y(t) = w_1(t) \sum_k f_1(x_k(t), \tau_k) + w_2(t) \sum_k f_2(x_k(t), \tau_k)$$

$$f_k(x) \sim N(\mu, Q^{-1})$$

where w_k is are the weights of each catalogue,
Q is the sparse precision matrix, and $\mathrm{Q} = \sum^{-1}$.

4.2 the INLA method

The main method used in this thesis is called “INLA” on integrated nested Laplace approximation, which is method for approximate Bayesian inference. It is implemented in the R language R-INLA package. Compared with some general inference such as Monte Carlo Markov chain, INLA is a simpler and quicker alternative that can achieve similar numerical accuracy for specific models. In addition, INLA methodology includes but is limited to latent Gaussian Markov Random Field (GMRF) models.

4.2.1 the Bayesian method

To simulate the random walk mentioned in section 4.1.4, a prior distribution should be specified at first, such that the corresponding posterior distribution can be obtained. This process makes essential qualification between unknown and observed quantities and is called Bayesian inference. And the INLA method allows us to define the prior of the hyperparameters in a variety of methods.

Let θ be the generic parameter, the likelihood function is written as:

$$L(\theta) = p(Y = y|\theta)$$

While the random variable Y is modeled with probability distribution or density function respectively under different conditions of discrete or continuous. The distribution of Y depends on θ.

The posterior distribution $p(\theta|y)$ is as follows:

$$p(\theta|y) = \frac{p(y|\theta)p(\theta)}{p(y)}$$
$$\propto p(y|\theta)p(\theta)$$

where $p(y)$ refers to the marginal distribution of the dataset. Besides, as a normalization constant, $p(y)$ is independent of θ, thus the proportion is established. $p(y|\theta)$ is recognized as the likelihood.

When extending to the condition of discrete values in θ, the process of marginalizing $p(y)$ could be thought as:

$$p(y) = \sum_{\theta \in \Theta} p(y|\theta)\, p(\theta) \text{ , when } \theta \text{ is discrete}$$

$$p(y) = \int p(y|\theta)p(\theta)\, d\theta \text{ , when } \theta \text{ is continuous}$$

where Θ are the aggregate of all possible values which θ can assume.

4.2.2 Laplace approximations

When considering of the Laplace approximation, which could also be thought of as the Taylor series expansion. In another word, doing the Laplace approximation, actually we are calculating a Taylor expansion. Suppose we have a point a, thus it could be expanded into a form of sum of lots of terms. Then an approximation could be served by using a finite number of terms as in the equation below.

$$f(x) = f(a) + \frac{f'(a)}{1!}(x-a) + \frac{f''(a)}{2!}(x-a)^2 + \frac{f'''(a)}{3!}(x-a)^3 + \cdots$$

To approximate any PDF with a gaussian distribution, the Laplace approximation could be used. While to estimate the mode $\hat{x}$ of a function, it always takes the first three terms in the Taylor series expansion. In other word, the first three terms of the Taylor expansion are generally taken into calculation, up to the second derivative. The log differentiation $\log g(x)$ function calculated from the Taylor expansion could be expressed as:

$$\begin{aligned}\log g(x) &\approx \log g(\hat{x}) + \frac{\partial \log g(\hat{x})}{\partial x}(x-\hat{x}) + \frac{\partial^2 \log g(\hat{x})}{2\partial^2 x^2}(x-\hat{x})^2 \\ &\approx \log g(\hat{x}) - \frac{1}{2\sigma^2}(x-\hat{x})^2\end{aligned}$$

where the variance is estimated with the foundation of curvature $\hat{\sigma}^2 = -(\frac{\partial^2 \log g(\hat{x})}{2\partial x^2})^{-1}$. With the increasing of the degrees of freedom, the approximation will become better and better. And the hierarchical model mentioned in former subsection could be fitted by replairy the hand to compute $p(y)$ with it is approximate Gaussian..

When the above function has been solved out for the Gaussian distribution, and as the ratio of g to $p(x|\theta, y)$ is a constant, the distribution of the desired posterior probabilities could be found. In addition, it should be noticed that the posterior probability from the point estimation method is a specific function of X, whereas the posterior probability from the Laplace approximation method is a random variable that follows a Gaussian distribution.

In summary, the Laplace approximation is an alternative method for computing posterior probabilities. It first assumes that the posterior probability $p(x|y)$ obeys a Gaussian distribution. Then, the log form of the function, which is constant compared to the posterior probability, is Taylor expanded at $\hat{x}$ to solve for this Gaussian distribution.

Once this Gaussian distribution is available, for each new sample, the expected value of this Gaussian distribution is calculated and is the prediction of the model for that new sample.

4.3 Time-series model

4.3.1 ARMA(p, q) process

Autoregression moving average process (ARMA) is one of the parametric families of stationary time-series. To some extent, the general methods for linear prediction are significantly simplified by using ARMA processes.

Suppose $\{X_t\}$ is stationary for every t value, then we consider $\{X_t\}$ as an ARMA(p, q) process with the notation:

$$X_t - \phi_1 X_{t-1} - \cdots - \phi_p X_{t-p} = Z_t + \theta_1 Z_{t-1} + \cdots + \theta_q Z_{t-q}$$

where $\{Z_t\} \sim WN(0, \sigma^2)$, $(1 - \phi_1 X_{t-1} - \cdots - \phi_p X_{t-p})$ and $(1 + \theta_1 Z_{t-1} + \cdots + \theta_q Z_{t-q})$ are polynomials that do not include common factors.

Simplify the notation of $(1 - \phi_1 X_{t-1} - \cdots - \phi_p X_{t-p})$ and $(1 + \theta_1 Z_{t-1} + \cdots + \theta_q Z_{t-q})$ to $\phi(z)$ and $\theta(z)$ respectively, the process could be written as the more concise form as:

$$\phi(B) X_t = \theta(B) X_t$$

where B is the backward shift operator:

$$B^j X_t = X_{t-j} \quad (j = 0, \pm 1, \ldots \ldots)$$

However, when considering the equation for ARMA process above, the process $\{X_t\}$ is stationary only if

$$\phi(z) = 1 - \phi_1 z - \cdots - \phi_p z^p \neq 0, \quad for \ \forall |z| = 1$$

4.3.2 ARIMA(p, d, q) process

Although the ARMA processes are representations of stationary series, the autoregressive integrated moving average model (ARIMA) is introduced to account for non-stationary conditions. There are many kinds of non-stationarity. one typical thing is to have a long-term trend. The next option is to have a periodic trend that used to have some stochastic variation around some periodic signals.

$\{X_t\}$ is thought to be an ARIMA (p, d, q) process, where "I" refers to the integrated with some differencing Y_t. Define $Y_t = (1 - B)^d X_t$ is a stationary ARMA (p, q) process, where d is a nonnegative integer.

When the difference is combined with the autoregressive models with the moving

average model, a non-seasonal ARIMA model as below could be obtained.

$$y_t' = c + \phi_1 y_{t-1}' + \cdots + \phi_p y_{t-p}' + \theta_1 \varepsilon_{t-1} + \cdots + \theta_q \varepsilon_{t-q} + \varepsilon_t$$

where y_t' is a sequence that could be differenced several times. To simplify the process, it could also be thought as:

$$\left(1 - \phi_1 B - \cdots - \phi_p B^p\right)(1 - B)^d y_t = c + (1 + \theta_1 B + \cdots + \theta_q B^q)\varepsilon_t$$

(Hyndman and Athanasopoulos, 2018)

Generally, there are three main steps when doing the time-series simulation. First and foremost, as data being stationary is one of the important assumptions of ARMA models, a model accounts for long-scale structure should be fitted to the data. Secondly, determine the order of the model based on autocorrelation and partial correlation. The final step is to build model and test.

4.4 Time-series estimation with ACF and PACF

The autocorrelation function (ACF) illustrates how the current value in a given time-series process is correlated to the previous values. While the partial autocorrelation function (PACF) explains the partial correlation between the sequence and its own lags.

These two give measurements are needed to decide the model order that should be fitted to the data. The comparison between the ACF and PACF of AR, MA, ARMA models are shown in the table 4.4.1 below.

Table 4.4.1: Characteristics for the autocorrelation functions

	ACF $\rho(k)$	PACF ϕ_{kk}
AR(p)	Damped exponential or/and sine function	$\phi_{kk} = 0 \; for \; k > p$
MA(q)	$\rho(k) = 0 \; for \; k > q$	Dominated by damped exponential or/and sine functions
ARMA(p, q)	Damped exponential or/and sine functions after lag $q - p$	Dominated by damped exponential or/and sine functions after lag $q - p$

4.5 The validation method

4.5.1 DIC criterion

For any data set, modelers will face the problem of model selection. Especially for many complex models, identification has always been a difficult problem. DIC is a simple but efficient method, which was proposed by Spiegelhalter in 2002, to do the model comparison.

Suppose that the distribution of data observation $Y = (y_1, \dots\dots, y_n)$ depends on a p-dimension parameter vector. $f(y|\theta)$ represents the log likelihood function, and $g(\theta|y)$ is posterior distribution. Then the DIC could be expressed as:

$$DIC = 2E_{\theta|y}[-2\ln f(y|\theta)] - (-2E_{\theta|y}[-\ln f(y|\bar{\theta})])$$

where the $E_{\theta|y}[X]$ refers to the mean value of X under the posterior distribution $g(\theta|y)$, and $\bar{\theta}$ is the posterior mean of θ.

Similar to the Akaike information criterion (AIC) and Bayesian information criterion (BIC) (the general conception of AIC and BIC is given in the appendix), the DIC criterion has also taken both the data fitting and the complexity of the model into consideration. However, the DIC criterion could compare complex statistical models very well. In other words, DIC is more suitable for models who have many unknowns.

According to the definition, DIC is the sum of deviance average $\overline{D}$ and penalty term $p_D = \overline{D} - \widehat{D}$, which indicates the distance between samples and reconstructions. p_D will become the number of parameter when the prior probability distribution flat enough.

As AIC, Akaike information comparison criterion, is a test of fit based on maximum likelihood. The calculating formula is written as the following:

$$AIC = 2k - 2\ln(\hat{L}) = D_{train} + 2p$$

where k is the number of estimated variables,

$\hat{L}$ the maximum value of the likelihood function,

p is the number of free parameters in the model.

It should be noticed that DIC is calculated from the posterior probability distribution of

the deviation of the training sample. Generally, we think that the deviation is only a MAP (maximum posterior probability) value of the distribution. Since DIC has an operation part that specifically expresses the flexibility of the model when fitting training samples, too much flexibility will lead to overfitting. $E_{\theta|y}\left[-\ln f(y|\bar{\theta})\right]$ is sometimes called a penalty term, which represents the distance between the deviation of the training sample and the deviation of the sample.

4.5.2 Watanabe-Akaike information criterion (WAIC)

Watanabe–Akaike information criterion (WAIC), or the widely applicable information criterion (Watanabe, 2010), is an extension version of the Akaike information criterion (AIC). Just as DIC, WAIC calculates the number of parameters to compensate for overfitting. However, compared to DIC, WAIC is a much more fully Bayesian comparison method. When comparing the fitted models, smaller WAIC value means better fit.

The WAIC is competed as the fitted model relates to the model complexity as:

$$WAIC = -2(lppd - p_{WAIC})$$

Where the model complexity could be shown as:

$$p_{WAIC} = \sum_{i=1}^{n} var(\ln\left(p(y_i|\theta)\right))$$

When calculating the WAIC, -2 times of the difference is chosen to use in order to keep it in the scale of deviance. This is the same conception as the original definition developed by Watanabe, "*WAIC is the negative of the average log pointwise predictive density*".

Chapter 5

Analysis and Results

5.1 Carbon dioxide flux and daily temperature change

According to the research published by Bridgham's group in 2006 and Mitsch's group in 2013, the absorption of carbon dioxide flux in most wetlands is affected by photosynthesis and respiration of vegetation in the regional ecosystem. What is more, there is a negative correlation between carbon dioxide flux and temperature in wetland or woodland ecosystems, since highly temperature gives more photosynthesis. (Halbedel, and Koschorreck, 2013; Gruca *et al*., 2017)

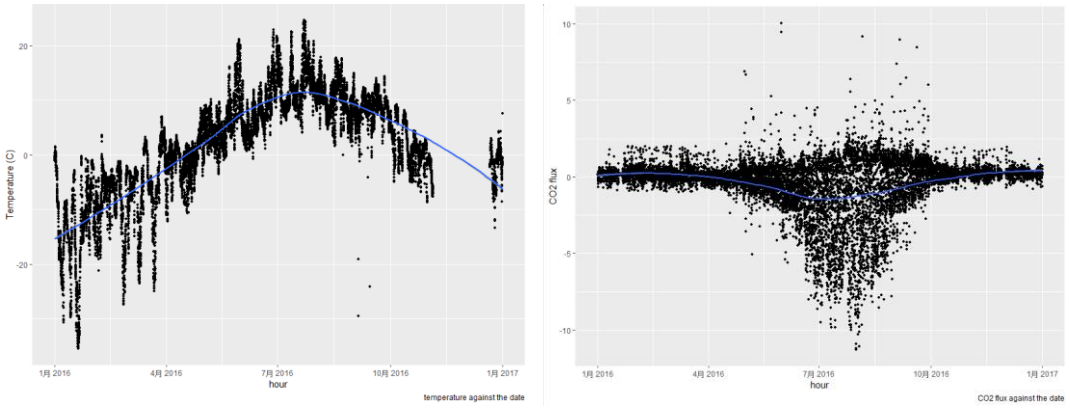

(a)temperature (b)carbon dioxide flux

Figure 5.1.1: temperature and carbon dioxide as a function of time

Figure 5.1.1 is plots of the yearly trend in air temperature and CO_2 flux. It could be easily seen that the CO_2 flux shows a negative correlation with the air temperature from the perspective of the overall trend throughout the year. With the summer coming and temperature rising, the general CO_2 flux becomes lower and more scattered within each day. However, it is not the same relationship over the year or seasons. Take two random days selected from winter and summer respectively for example, it seems that there's little relationship between the air temperature and the CO_2 flux during the winter.

Figure 5.1.2 shown below are the temperature and CO_2 flux against the time, which is calculated every half an hour. For the winter observation, January 24th was randomly chosen. As the blue line illustrates the change of air temperature and the red line expresses the CO_2 flux.

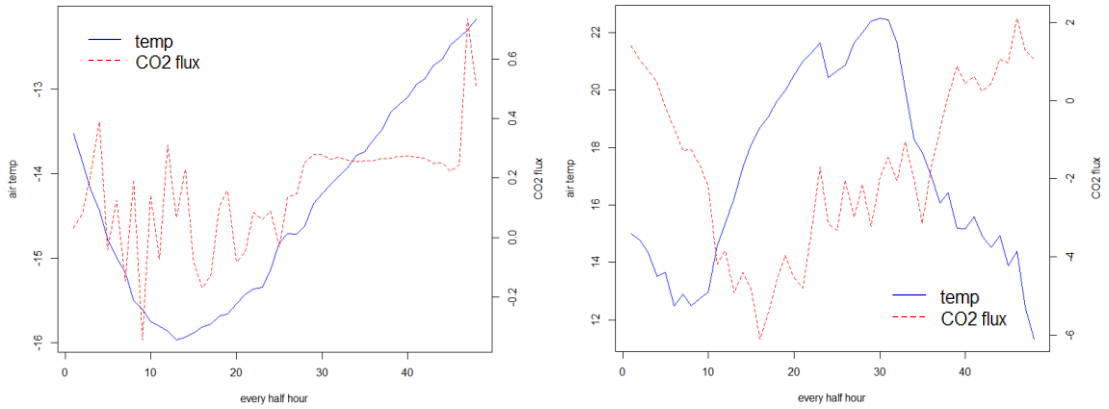

(a)a random day in winter (1.24) (b) a random day in summer (7.12)

Figure 5.1.2: temperature and carbon dioxide daily trend

In winter morning, the CO_2 flux shows some fluctuation before the time around 12:00am, but the volatility interval is small. After about 14:30pm, the CO_2 flux keeps at a stable and nearly constant level until around 22:00pm. However, the daily temperature during winter arrives at the lowest point at around 6:00 in the morning and starts to rise until 24:00 in the night. According to these two trends of CO_2 flux and temperature, there is little influence of temperature on the CO_2 flux, which may be because of the sustained low temperatures during the winter season.

On the other hand, when it comes to summer, it is obvious from the subfigure that the CO_2 fluxes and temperatures show opposite trends during most of the day. It is worth noting that during the summer there are long periods of the day. This maybe because of photosynthesis. Due to the lush growth of green leafy plants in summer and the long days and short nights during this season, there is plenty of sunlight and chlorophyll for photosynthesis in plants. As the result, much CO_2 is consumed, resulting in the negative fluxes.

5.2 Carbon dioxide flux and methane flux

The emission sources of methane (CH_4) mainly include natural wetlands, rice fields, natural gas spills, landfills, and biomass burning. Wetlands account for 70% of all natural CH_4 emissions and about 20% of global CH_4 flux. (Huai *et al*, 2006). However, CH_4 fluxes from wetlands have significant differences because of the different environments and vegetation types.

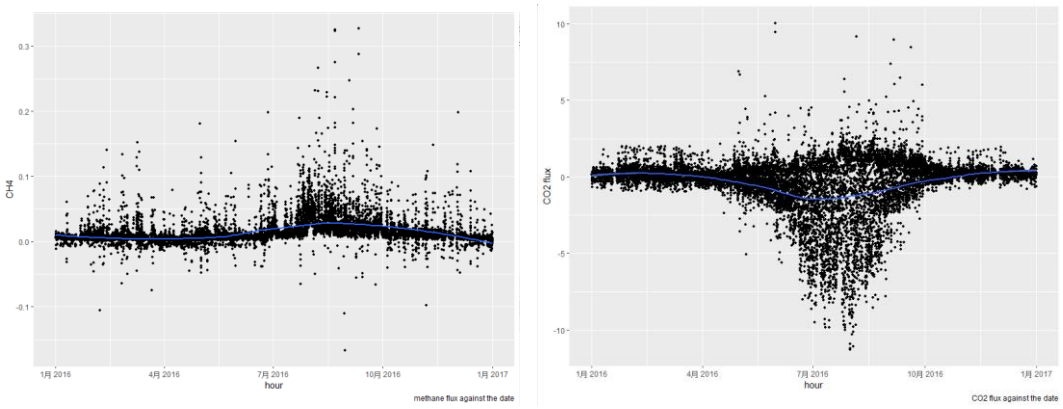

(a) methane flux (b)carbon dioxide flux

Figure 5.2.1: methane and carbon dioxide flux chart following time pace

Due to the low temperature in winter, the activity of methanogens decreases, and the CH_4 flux is close to zero (most of time smaller than 0.08 $g/m^2/h$). As the temperature increased in late spring, the activity of methanogens increased, and CH_4 flux begins to increase slightly. Additionally, there was a significant peak of CH_4 emissions at the end of August and early September, while the CO_2 flux would decrease to their lowest range at the same time period.

When looking at the single day trend of CH_4 and CO_2 flux, for the same two days as in Figure 5.2.2. The CH_4 flux during the winter always shows some fluctuates from midnight to the morning, while during other times in the day is stable enough although still has some small fluctuations. Moreover, the flux of methane and carbon dioxide has significant negative correlation during the summertime, except several time point, when the CH_4 flux value is particular high or low, such as the abnormal high peak at around 20:00 in the evening of June 24th.

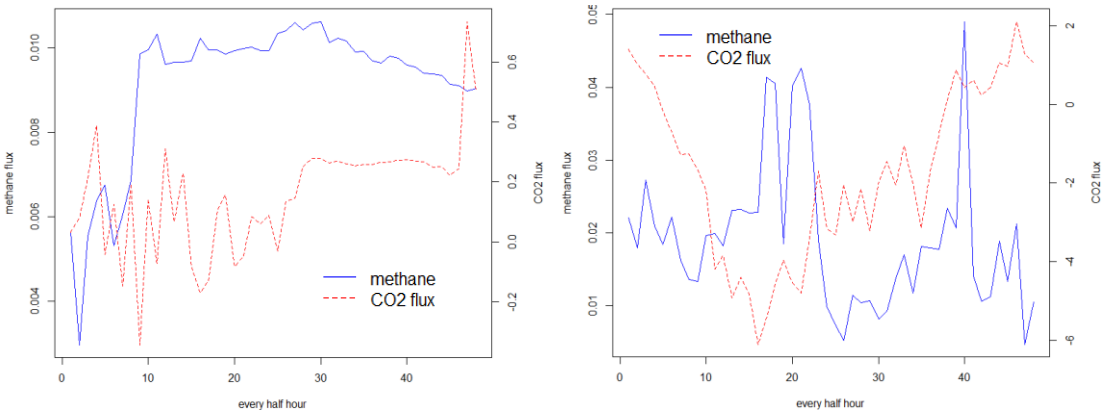

(a)a random day in winter (1.24) (b) a random day in summer (7.12)

Figure 5.2.2: flux of methane and carbon dioxide daily trend

Nevertheless, there is no direct way to see a significant interaction between CO2 and methane fluxes just from the graphs of the random two days belonging to different seasons.

5.3 Time-series pattern

When looking at the carbon dioxide flux observation plot, it shows evident circular mode. This may be the result of the seasonality that are thought to be significant influence. This is the reason why we use time unit effect as a time-series model with different time units in the later regression simulating.

5.3.1 The ACF and PACF

The study of data collected sequentially over time is referred to as time series analysis.

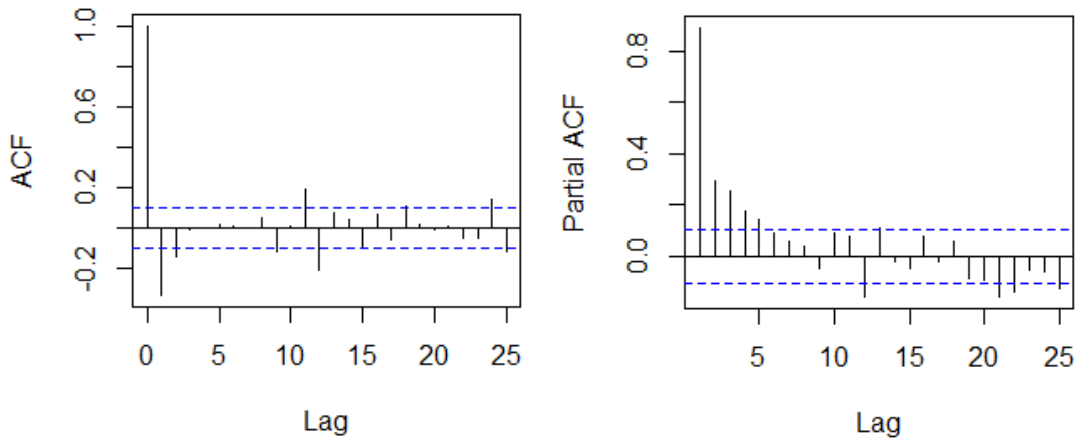

(a) autocorrelation function (b) partial correlation function

Figure 5.3.1: The acf and pacf for the CO_2 flux data, which are used to check and decide the lag and order of the day model.

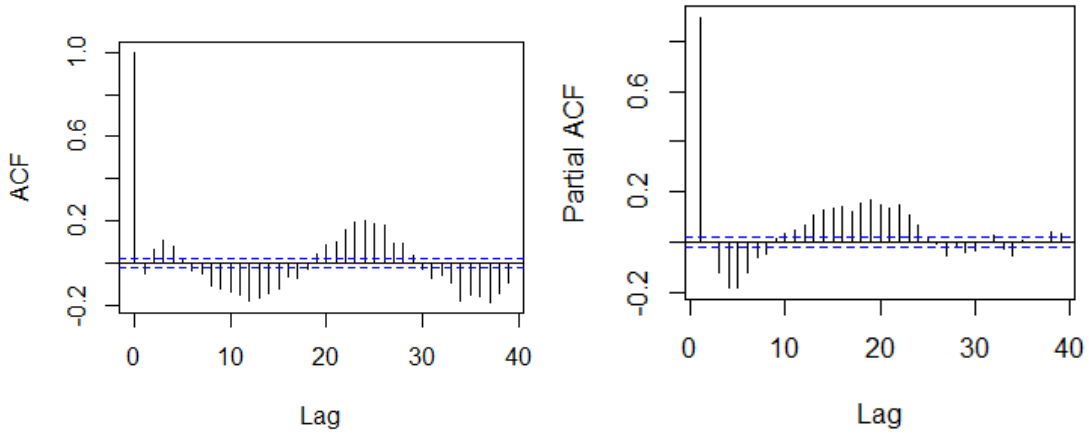

(a) autocorrelation function (b) partial correlation function

Figure 5.3.2: The acf and pacf for the CO_2 flux data, which are used to check and decide the lag and order of the hour model.

In order to estimate for different time units, the CO_2 flux data was calculated into daily average values and hourly average values when checking the autocorrelation and partial autocorrelation. It should be noticed that the new data files set for daily average and hourly average are just used for the stationary test and the AR process, integrated, and MA parts lags determination, which will be used for choosing the orders for different time units during the simulation.

5.4 The INLA model

In this step, the linear predictors are joined into a single model. By using the INLA method, estimated functions would not look like the general regression form, instead, they would be modeled as the formula shown below:

$$y(t) = w_1(t)\sum_k f_1(x_k(t), \tau_k) + w_2(t)\sum_k f_2(x_k(t), \tau_k)$$

where y refers to the CO_2 flux, fw_1 and fw_2 are the flux contributions from forest and wetland at each time respectively, $x_k(t)$ are the explanatory variables at each time, while τ_k are the parameters of the non-linear regression.

Moreover, the $w_1(t)$ and $w_2(t)$ are the weights for forest and wetland area respectively. f_1 and f_2 are the simulations for different variables $x_k(t)$. For most of the explanatory variables, temperature, humidity, heat flux and methane flux included,

f is simulated with random walk. However, for time units variables, day and hour included, f is simulated as AR(p)-process.

5.4.1 Reconstruction for each separate variable

As the original observations does not have the separate measurements for the fluxes coming from wetland and forest respectively, the reconstruction for each separate variables were adopted with the expectation of appropriately reducing the bias in the final model estimations. To start with several significant influenced factors for the mode, the means for the different parts and the variance for the latent field and observations for each single variable are plotted divided into two lines in accordance with the land type. (Figure 5.4.1)

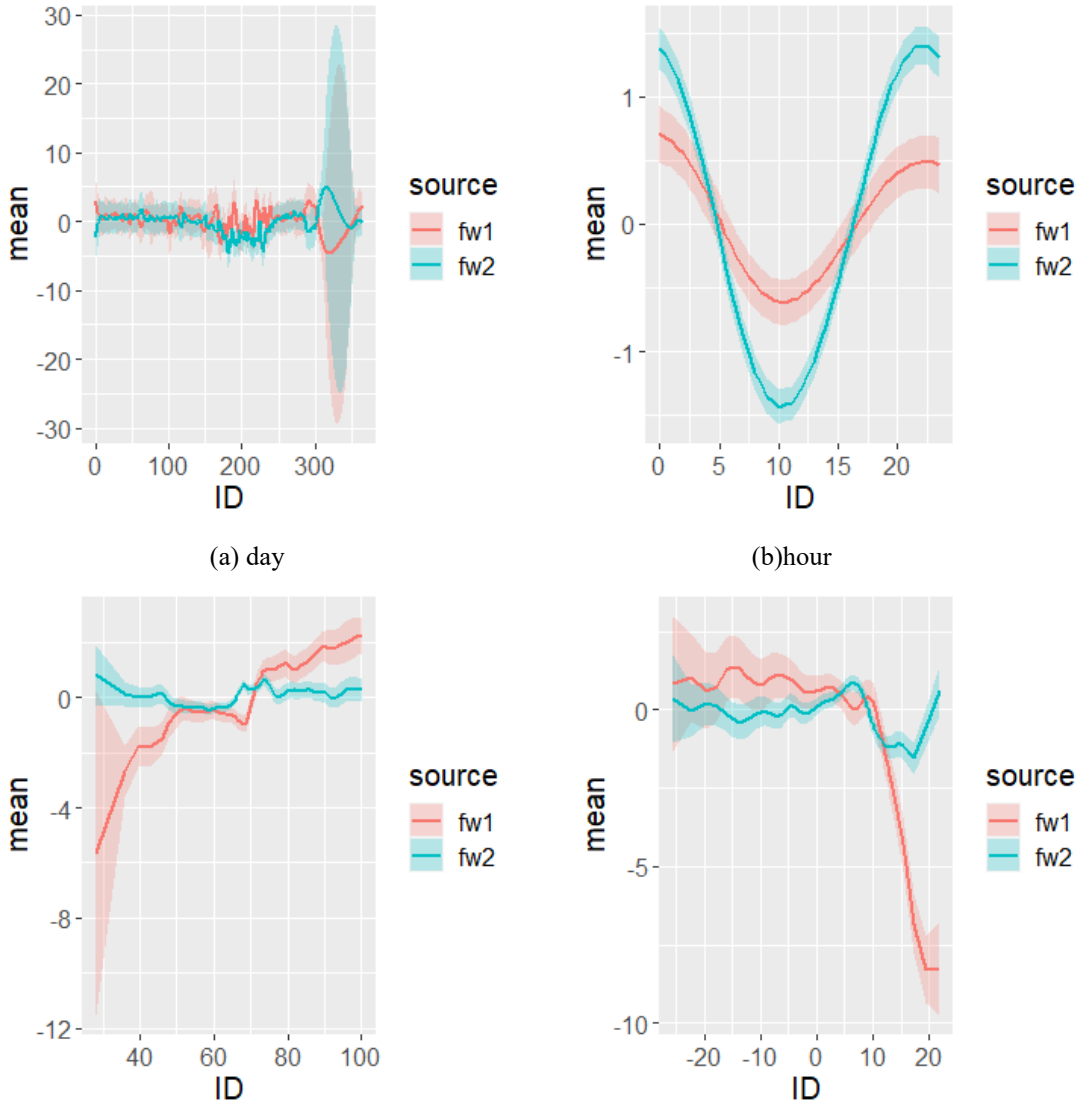

(a) day

(b)hour

(c) humidity

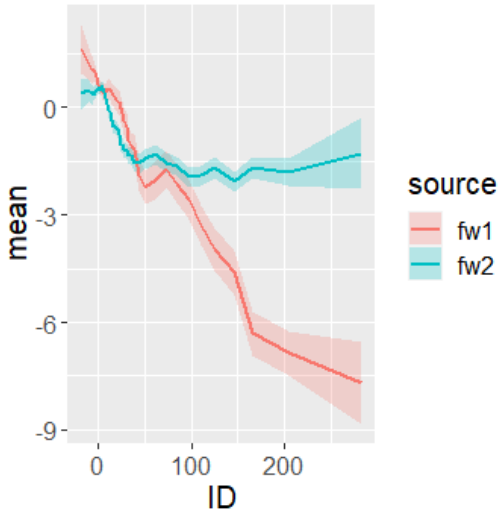

(d)temperature

(e) latent heat

(f)sensible heat

(g) methane flux

Figure 5.4.1: The reconstruction for each variable

In addition to the different time units used to model, the factors of humidity, temperature, heat, and methane flux would be considered as possible explanatory variables in the fitted models.

As the subfigures for sensible heat and latent heat shows similarly, the scatter plot, which is given in the Figure 5.4.2, is used to determine whether to use both heat variables or if just one of them should be chosen.

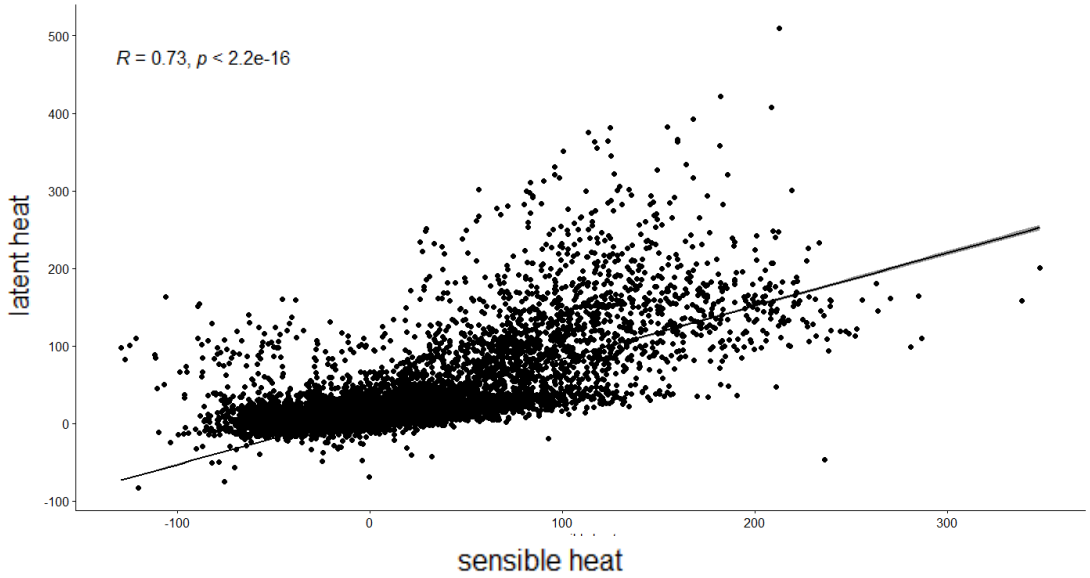

Figure 5.4.2: the correlation between sensible heat and latent heat

As can be seen from the figure above, the correlation between sensible heat and latent heat is 0.73. Moreover, the fitted function is close to a straight line over a large range, although there is some spread. By comparing the correlation of these with the CO_2 flux separately, only the factor of sensible heat used into the model.

5.4.2 the time series INLA model fitted with day unit

The AR order for the day parameter is chosen as 3 firstly, based on the ACF in section 5.3.1. However, when combined with other covariates the result shows non-significant for the PACF2 and PACF3 components, which means that the higher order may not be necessary. So, the order 1 for AR process is used during the modeling.

Parameters for the five models' considerations are presented in the Table 5.4.1, along with parameter estimates. We note that the mean value differs for the two CO_2 components, but the random walk precision is taken as common for each explanatory variables and the AR-process is taken for time unit variable.

Table 5.4.1: Non-linear regression parameters table for day models

		β_0	x1	x2	x3	x4	x5	x6
fit1	fw1	-0.44	1.18	0.48	25.95	75.01	0.069	109.33
	fw2	-0.25						
fit2	fw1	-0.52	1.10	0.51			0.058	104.23
	fw2	-0.26						
fit3	fw1	0.43	0.63	0.26	11.66	44.75		
	fw2	-0.78						
fit4	fw1	0.53	0.67	0.23	11.59	62.72	0.031	
	fw2	-0.79						
fit5	fw1	-0.47	1.08	0.35	20.85	38.20		145.92
	fw2	-0.20						

Notation: the parameters for non-linear regression from x_1 to x_6 refer to: the precision for Gaussian observations, day, temperature, humidity, CH4, and sensible heat flux in order.

Table 5.4.2. DIC and WAIC comparison

	fit1	fit2	fit3	fit4	fit5
DIC	30763.4	31454.2	37573.2	37045.1	31647.3
Saturated DIC	19343.3	20034.2	26153.1	25625	20227.2
WAIC	-17553.8	-17538.9	-19850.6	-20432.2	-16877.5

Notation: the models' name in this table are the same model as in Table 5.4.1.

In order to have a more intuitive and clearer model measurement and comparison standard, the DIC criterion is used, and the result table is shown above as Table 5.4.2 for the same models in Table 5.4.1. According to Spiegelhalter (2002), if the difference between the DIC of the two models is greater than 10, the model with the smaller DIC is better. In contrary, if the difference between the DIC of the two models is less or equal than 5, it means that there is not much difference between the two models. As a result, depending on the DIC, the model including temperature, humidity, methane flux and sensible heat flux shows a better result, the DIC of which equal to 30763.4

The WAIC results show a little bit different within the model selection when compared with DIC. The better fitted model following WAIC values is the one that includes variables of temperature, humidity, and sensible heat flux, whose WAIC is

equal to -16877.5. The condition that selections of model does not exactly match under the two validation methods is possible. Because DIC is based on the posterior mean $\mathrm{E}[\theta|y]$ and just get a single value for each model. Nevertheless, WAIC uses the log predictive density as the core idea and has the validation values for each time point before doing the average for whole models.

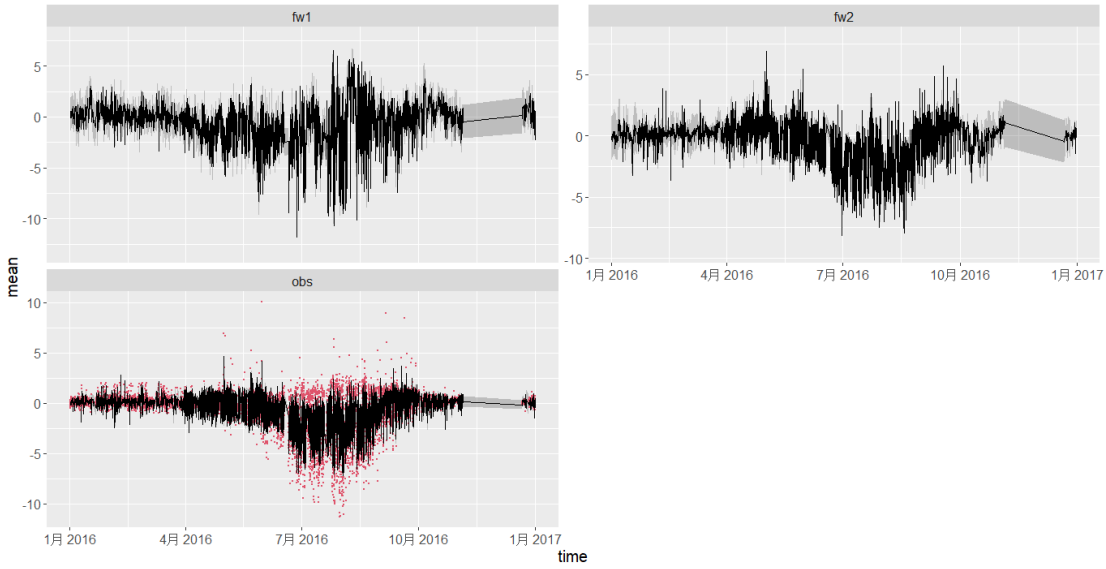

(a) all data along with points matching the reconstruction, with data for forest and wetland separately and without the land type classification

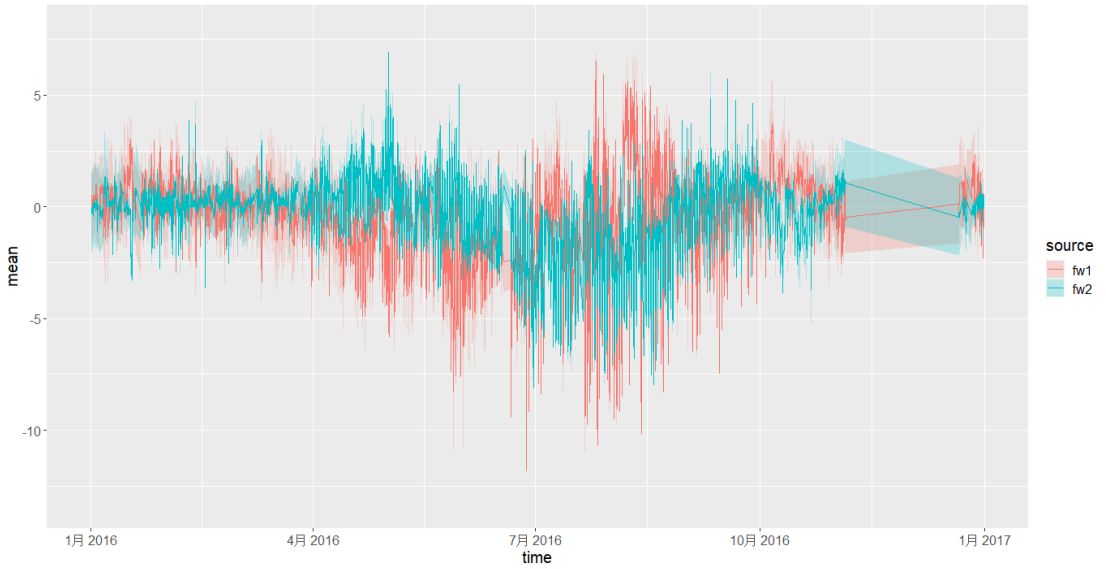

(b) the reconstruction values in the same figure for comparison

Figure 5.4.3: the observations values and reconstruction values fitted with land type

5.4.3 the time series INLA model fitted with hour unit

Before the differential step, the ACF and PACF function diagram for the hourly unit dataset shows significant periodogram around 22, which is reasonable as in this hourly dataset every 24 values are the data for whole day. After using differentiation to reduce the impact, MA order is still high. To deal with this, the high order for AR process is used to compensate for the MA process at first. But the order reduced to 3 after checking the significance.

Table 5.4.3: posterior summary table for parameters for hour

		β_0	x1	x2	x3	x4	x5	x6
fit1	fw1	0.005	0.87	5.98	15.53	1024.22	0.033	124.31
	fw2	-0.25						
fit2	fw1	-0.03	0.77	15.19			0.05	102.7
	fw2	-0.298						
fit3	fw1	0.01	0.32	0.60	1.19	5.34		
	fw2	-0.28						
fit4	fw1	0.27	0.62	2.38	5.81	304.19	0.03	
	fw2	-0.45						
fit5	fw1	-0.21	0.76	18.49	15.57	486.76		117.37
	fw2	-0.17						

Notation: the parameters for non-linear regression from x_1 to x_6 refer to: the precision for Gaussian observations, day, temperature, humidity, CH4, and sensible heat flux in order.

Table 5.4.4. DIC and WAIC comparison

	fit1	fit2	fit3	fit4	fit5
DIC	33793.2	35198.5	37939.9	37374.7	35289.2
Saturated DIC	22373.2	23778.5	26519.8	25954.7	23869.1
WAIC	-18862.4	-18987.2	-19693.1	-20158.2	-18305.6

Notation: the models' name in this table are the same model as in Table 5.4.3.

The same as daily unit models, validation of WAIC and DIC still shows a small difference with the hourly model selection. According to DIC, the model including variables of temperature, humidity, methane flux, and sensible heat flux is a better choice with the DIC equal to 33793.2. While the model including temperature, humidity,

and sensible heat flux is thought as a better selection depending on WAIC, which is equal to -18305.6.

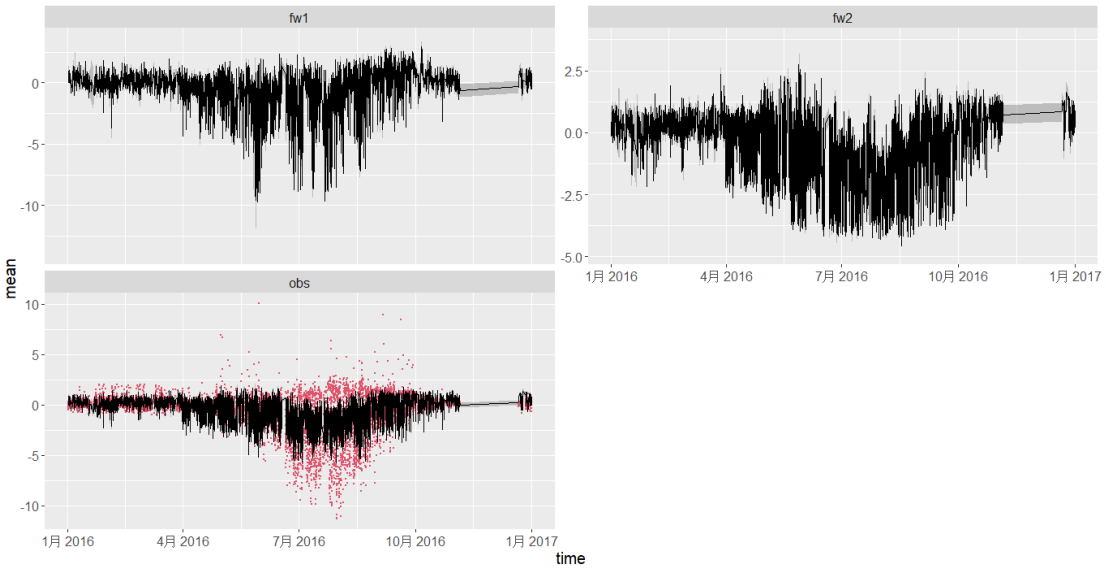

(a) all data along with points matching the reconstruction, with data for forest and wetland separately and without the land type classification

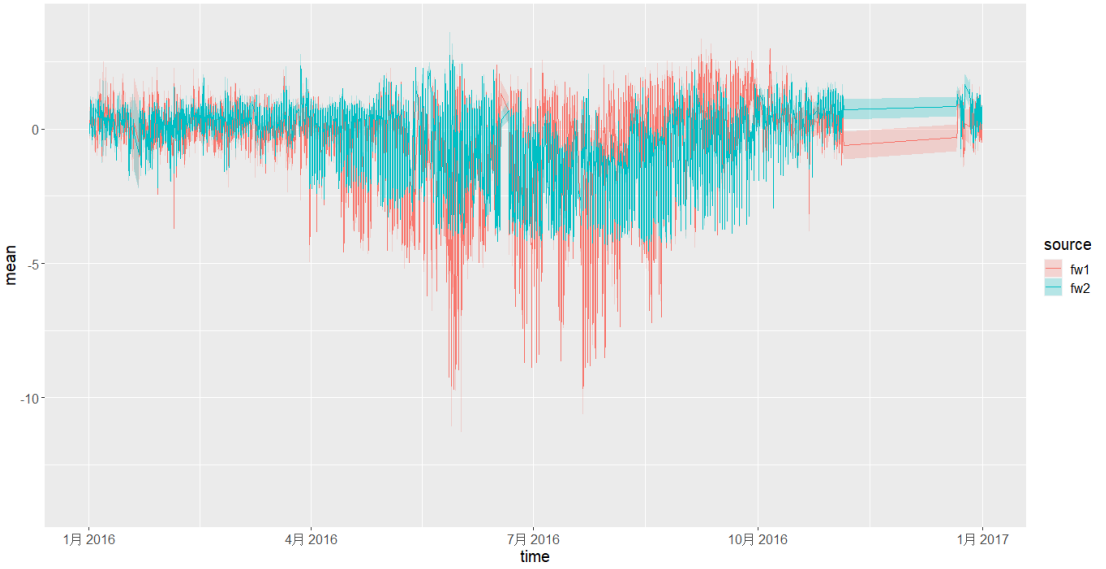

(b) the reconstruction values in the same figure for comparison

Figure 5.4.4: the observations values and reconstruction values fitted with land type

Chapter 6

Conclusion and Discussion

6.1 Conclusion

This study uses data from a eddy covariance system and micro-meteorological observations of meteorological factors such as methane and carbon dioxide fluxes in the Abisko national park. In view of the relationship between carbon dioxide flux and methane flux, air temperature, relative humidity, latent heat, sensible heat flux, and different temporal scales, the following points are summarized.

1. The carbon dioxide flux observation results show that the flux range in autumn, winter and early spring is between -1.3~2.5 μmol/m^2/s. Since the end of April, the range became larger and larger and reached a maximum range in late July and August. During the summertime, most of time the flux fluctuated in the range from -11.8 μmol/m^2/s to 7.5 μmol/m^2/s, while there's several time point when the flux has reached at around 9.2 μmol/m^2/s.

2. The carbon dioxide flux observation results show that the peak of methane flux occurs in late summer and early autumn, while the smallest change in the flux is during the winter. Taking the process of methane production into account, the low temperature of the Abisko wetland during the winter cause the methane transmission to be lower. Temperature rises in late spring and early summer, result in the increasing of methanogens activities. Then the CH_4 flux begins to rise.

3. There is a negative correlation between carbon dioxide flux and air temperature. During the summer, the CO_2 flux has obvious daily changes. Besides, there is a high correlation between carbon dioxide flux and heat flux. The flux during the summertime is much lower than the flux during the winter. This may because that the absorption of CO_2 by large areas of vegetation and forest in Abisko wetland during the summer is significant, resulting in a negative value of the flux during the day in summer. In addition, due to the few human activities, the CO_2 production in Abisko wetland in winter comes mostly from soil microbial respiration, and its value is much lower and even close to zero.

4. The model with time periodogram considered in is significantly better. In other words, there is a strong temporal variability in carbon dioxide flux. Especially when implementing seasonal changes into the parameters, it can better enable the model to simulate the observed data patterns. However, since there is no clear distinction between the dry season and the rainy season at Abisko, the seasonal influence is mainly reflected in the temperature and the resulting methane flux and heat flux.

5. In incorporating the time series model into the INLA model, both models for daily or hourly use the order of the AR process with higher values to compensate and override the order of the MA process with Markov structure, although these orders are replaced by lower value according to the significance test.

6. From the DIC and WAIC values, the model including all six variables is the best for both daily and hourly unit simulation. Besides, the comparison of these two validation methods between models using different time unit shows that the models estimated using days as the unit of time generally fit slightly better than the models estimated using hours as the unit of time.

6.2 Discussion and consideration

However, there are still some problems and disadvantages and need to be further study.

1. Due to the lack of distinction between training sets and validation set in the estimated model, the reconstruction might look small different and a little bit better from the actual result.

2. The carbon dioxide flux analysis focused on in this study is only limited to the exchange of surface gas but does not take the carbon balance of the entire net ecosystem into consideration. Therefore, the dissolved organic carbon and inorganic carbon in the landform water are not taken into consideration.

3. Because of the absence of exacta data for wetland and forest carbon dioxide respectively, it becomes difficult to test the validation of the estimation results. Although the reconstructions of all single variables are established before the

variables' selection, which could improve the model to some extent, there is still no definitive measure of how effective the model is.

4. As DIC and WAIC are expansions of AIC and BIC validation methods that are always used to test general regression models, they are more suitable for some complicated models. However, this thesis has not studied for the proving the goddess and showing how does DIC and WAIC better than AIC and BIC.

5. In the validation part, only the reconstruction for improvement and the validation criterions for the effective test. There is no confidence intervals to corroborate and supplement the results.

Bibliography

Alan E., Peter J. D., Montserrat F., and Peter G. (2010). Handbook of modern statistical methods: Handbook of Spatial Statistics. pp 172-174

Angrist J. D., & Pischke J. S. (2008). Mostly Harmless Econometrics: An Empiricist's Companion. Princeton University Press. Chapter 1.

Aubinet M., Grelle A., Ibrom A., Rannik U., Moncrieff J., Foken T., Kowalski A. S., Martin P. H., ¨Berbigier P., Bernhofer C., Clement R., Elbers J., Granier A., Grunwald T., Morgenstern K, Pilegaard K, Rebmann C, Snijders W, Valentini R, and Vesala T. (2000). Estimates of the annual net carbon and water exchange of forests: the EUROFLUX methodology. Adv Ecol Res 30, pp 113–175.

Baldocchi D.D., Eva F., Lianhong G., Richard O., David H., Steve R., Peter A., Bernhofer Ch., Kenneth D., Robert E., Jose F., Allen G., Gabriel K., Beverly L., Xuhui L., Yadvinder M., Tilden M., William M., Walt O., K. T. Paw U., Kim P., Schmid H. P., Riccardo V., Shashi V., Timo V., Kell W., and Steve W. (2001). FLUXNET: A new tool to study the temporal and spatial variability of ecosystem-scale carbon dioxide, water vapor, and energy flux densities. Bulletin of the American Meteorological Society, 82(11), pp 2415-2434.

Baldocchi D., Detto M., Sonnentage O., Verfaillie, J., Silver W., and Kelly N. M. (2012). The challenges of measuring methane fluxes and concentrations over a peatland pasture. Agricultural and Forest Meteorology. Vol.153, pp 177-187.

Baldocchi D., Hicks B., and Meyers, T. (1988). Measuring biosphere-atmosphere exchanges of biologically related gases with micrometeorological methods. Ecology 69, pp 1331-1340.

Bridgham S. D., Cadillo Q. H., Keller J. K., Zhuang Q. L. (2013). Methane emissions from wetlands: biogeochemical, microbial, and modeling perspectives from local to global scales. Global Change Biol 19, pp1325-1346

Brut A., Legain D., Durand P., Laville P., (1998). A relaxed eddy accumulator for surface flux measurements on ground-based platforms and aboard research vessels. American Meteorological Society, 21, pp 411-427.

Carl E. R., and Christopher K. I. W. (2006). Gaussian Processes for Machine Learning.

Dave C., and Louis S. (2018). Measuring gases using eddy covariance.

Denmead O. T. (2008). Approaches to measuring fluxes of methane and nitrous oxide between landscapes and the atmosphere. Plant Soil 309, pp 5-24.

Detto M., Verfaillie J., Anderson F., Xu L., and Baldocchi D. (2011). Comparing laser-based open- and close-path gas analyzers to measure methane fluxes using the eddy covariance method. Agricultural and Forest Meteorology. Vol. 151, pp 1312-1324

Gelman A., Carlin J.B., Stern H.S., Dunson D.B., Vehtari A., and Rubin D.B. (2014). Bayesian Data Analysis. CRC Press: Boca Raton, FL.

Gelman A., Hwang J., and Vehtari A. (2014). Understanding predictive information criteria for Bayesian models. Statistics and Computing, Vol 24, pp997-1016.

Gruca R. R., Bartoszek L., and Koszelnik P. (2017). The influence of environmental factors on the carbon dioxide flux across the water-air interface of reservoirs in south-eastern Poland. Journal of Environmental Sciences, 56, pp 290-299

Gubner John A. (2006). Probability and Random Processes for Electrical and Computer Engineers. Cambridge University Press. p441.

Halbedel S., and Koschorreck M. (2013). Regulation of CO2 emissions from temperate streams and reservoirs. Bio-geosciences 10(11), p7539.

Huai Ch., Shun Zh., Ning W., Yanfang W., Peng L., and Fusun Sh. (2006). Research progress on the production, oxidation and emission flux of wetland methane. Applied and Environmental Biology 12(5), pp 726-733

Hyndman, R.J., and Athanasopoulos, G. (2018) Forecasting: principles and practice, 2nd edition.

Joon K., Guirui Y., Akira M. (2010). AsiaFlux - sustaining ecosystems and people through resilience thinking. Observing, Predicting and Projecting Climate Conditions. pp 165-168.

Lee X., W. Massman, and Law B. (2004). Handbook of Micrometeorology. Kluwer Academic Publishers. The Netherlands. p250.

Legendre A. M. (1805). New methods for the determination of the orbits of comets, Firmin Didot, Paris. “Least Squares Method” appears as an appendix.

Lewickia J. L., Fischerb M. L., and Hilleyc G. E. (2007). Six-week time series of eddy covariance CO_2 flux at Mammoth Mountain.

California: performance evaluation and role of meteorological forcing

Lucy R., Timothy C. H., Clement S., Lukas S., Benoit B., Joana Z. C., Stephane P., Damien B., Patrick M., and Mathew W. (2014). Evidence for strong seasonality in the carbon storage and carbon use efficiency of an Amazonian Forest, Global Change Biology, Vol 20(3), pp979-991.

Marta B., and Michela C. (2015). Spatial and Spatio-temporal Bayesian Models with R-INLA.

Millar R. B. (2009) Comparison of hierarchical Bayesian models for overdispersed count data using DIC and Bayes' factors. Biometrics, 65, pp 962-969.

Mitsch W. J., Bernal B., Nahlik A. M., Mander U. L., Zhang L., Anderson C. J., Jorgensen S. E., and Brix H. (2013) Wetland, carbon, and climate change. Landscape Ecol, 28, pp 583-597.

Moncrieff J. B., Massheder J. M., DeBruin H., Elbers J., Friborg T., Heusinkveld B., Kabat P., Scott S., Sogaard H., and Verhoef A. (1997). A system to measure surface fluxes of momentum, sensible heat, water vapor and carbon dioxide. pp 188–189, and pp 589–611.

Moncrieff J. B., Valentini R., Greco S., Seufert G., Ciccioli P. (1997). Trace gas exchange over terrestrial ecosystems: methods and perspectives in micrometeorology. J Exp Bot 48, pp1133– 1142.

Morin T. H., Bohrer G., Stefanik K. C., Rey-Sanchez A. C., and Mathent A. M. (2017). Combining budget from a small, heterogeneous urban floodplain wetland park. Agricultural and Forest Meteorology. Vol 237, pp 160-170.

Moriwaki R., and Kanda M. (2004). Seasonal and Diurnal Fluxes of Radiation, Heat, Water Vapor, and Carbon Dioxide over a Suburban Area. Journal of Applied Meteorology and Climatology, Vol 43, pp 1700-1710.

Paul A. K. (2010). Wetland Ecology: Principles and Conservation. p2.

Pumpance J., Kolari P., and Ilvesniemi H. (2004). Comparison of different chamber techniques for measuring soil CO_2 efflux. Agricultural and Forest Meteorology. Vol 123, pp 159-176.

R-INLA Project. http://www.r-inla.org.

Rue H., Martino S., and Chopin N. (2009). Approximate Bayesian inference for latent Gaussian models by using integrated nested Laplace approximations. Journal of the Royal Statistical Society: Series B (Statistical Methodology) 71(2), pp319-392.

Spiegelhalter D. J., Best N. G., Carlin B. P., and Linde A. (2002). Bayesian measures of complexity and fit. Journal of the Royal Statistical Society, Series B 64, pp 583-639.

Timothy C. H., Edmund R., and Mathew W. (2012). The use of CO2 flux time series for parameter and carbon stock estimation in carbon cycle research. Global Change Biology, Vol 18(1), pp 179-193.

Tongbao L., Zhiqiang W., Xuelei S., Yiwei Q., and Zhanying M. (2008). CO2 Flux and Impact Factors in Winter Wheat Field Ecosystem. Chinese Journal of Eco-Agriculture. Vol 16(6), pp 1458-1463.

Verma S. B. (1990). Micrometeorological methods for measuring surface fluxes of mass and energy. Remote Sensing Reviews 5(1), pp 99-115.

Wackernagel H. (2003). Multivariate Geostatistics. Springer.

Watanabe S. (2010). "Asymptotic Equivalence of Bayes Cross Validation and Widely Applicable Information Criterion in Singular Learning Theory". Journal of Machine Learning Research. 11: pp 3571–3594.

Xuguang T., Zongming W., Jing X., Dianwei L., Ankur R. D., Mingming J., Zhangyu D., Xiuping L., and Bo L. (2013) Monitoring the seasonal and interannual variation of

the carbon sequestration in a temperate deciduous forest with MODIS time series data, Forest Ecology and Management, pp150-160.